Noise and Vibrations Reduction of Stone Cutting Factories

Ahmed Abu Hanieh*[a], Ahmad Al Balasie[b]

[a,b] Birzeit University, PO Box 14, Birzeit, Palestine.
[a]ahanieh@birzeit.edu, [b]abalasie@birzeit.edu
*Corresponding author, ahanieh@birzeit.edu

***Abstract*-- This research handles the problem of noise pollution caused by the stone cutting processes in the medium and small factories located close to the populated areas. Noise can be reduced by two main ways: the first method is done by adding sound absorbers to the workshop surrounding walls; the second technique is by building a barrier wall in front of the open facade of the factory. This paper introduces three techniques to reduce the vibration in the stone cutting machine knowing that vibration is the main source of noise, the techniques are: inserting a passive elastomeric rubber pad, designing an active controller based on Integral Force Feedback (IFF), and designing a regulator based on Linear Quadratic Regulator (LQR) for active control of vibrations. Simulation results show the ability of these techniques to regulate the vibrations at various levels.**

***Index Term*-- stone cutting; noise reduction; sound pressure level; sound absorber; LQR; IFF.**

1. INTRODUCTION

Stone cutting factories are considered one of the dramatic sources of noise in populated areas. In the mediterranean region, for example, small and medium stone factories spread amongst the populated houses. Cutting machines in these factories rotate at high speeds where the vibration induced by the impact between the cut stone and the cutting teeth produces a high-frequency sound, this sound confirms a source of noise, headache and pain for neighbourhood houses in the vicinity of the factories (Jaber et al., 2015). The level of noise generated by stone cutting reaches up to the level of noise generated by drills used in the ear surgery that ranges from 88 – 108 dB as discussed in refrenece (Kylen et al., 1977) which is painful and can cause damage to the human hearing system. Occupational safety of stone cutting was discussed by Aleksandrova and Timofeeva (2017) where the authors study the stone cutting profession as a high occupational risk profession, specifying the risk indicators by the assessment of the risk related to workers in this sector. Senior researchers from the University of Southampton worked on using active isolation of the vibrations induced by rotating machinery like stone cutting machines in (Jenkins et al., 1993). The secondary force was used in parallel to the passive vibration isolation to form a hybrid active-passive technique to isolate the vibrations of rotating machinery in this reference which improved the performance of the isolation system. Other researchers from MIT applied the active narrowband controller to reduce the noise induced by the resonant substructures in vibrating machinery (Skribner et al., 1993). Nevertheless, noise is not always a drawback, on the contrary, it has some benefits that researchers can use for obtaining specific information. Noise level and frequency coming from stone cutting varies from one type of rock to another and depends on the physical and mechanical properties of these rocks, Delibalta et al., (2015) investigated the usability of noise level produced by cutting of rocks to predict the mechanical and physical properties of these rocks. The sound radiated by the rotating stone cutting machines is spread in three ways; the first is through the open main front of the factory and this can be solved by adding a sound retention barrier at a certain height and distance from the source of the sound, the second is through the other three walls of factory hanger or building and this can be solved by lining the internal side of the building walls with a sound isolation material at a specific design and thickness, the third way of noise transmission is by propagating from the machine body through the concrete floor to the workers and surrounding environment (Jeon et al., 2002). The problem of sound isolation in acousto fluidics was used a long time ago by implementing metallic noise isolation tubes made of Barium Titanate material to avoid the propagation of ultrasonic waves (Sykes and Harrison, 1952). Others concentrated on using lead sheets as a ceiling barrier of sound for lightness and mechanical properties (Goodfriend, 1993).

Sound noise is considered a pollution source because it causes air pollution that leads to health problems. Sound is not the only pollutant produced by stone cutting, other effects are transferred to the environment through the stone industry; these effects vary from rock mining, dust, and soil contamination (Al-Joulani, 2008). Another important study of the environmental effect of stone cutting processes is tackled in Sayara (2016). Using Barriers is one of the solutions to isolate noise, this idea has been used widely to isolate the noise of vehicles and trucks on the highways from transmitting to the

neighbourhood houses (Jie et al., 2017), this technique will be used later to isolate the noise of stone cutting machines.

2. Noise Pressure Level Measurements

Noise is the unwanted level of sound created by vibrating elements causing sound waves transmitted by air. These waves have a specific frequency that depends on the frequency of mechanical vibration (dynamic motion) that generates this wave and distributes it into the air, the audible range for a normal human being varies from 20 Hz to 20 kHz (ASHRAE, 2020). The wave also has an amplitude called sound pressure level and measured in decibels (dB) to be represented in a logarithmic scale in powers of 10. The sound pressure level is calculated by Eq. (1):

$$L_p = 20\ log_{10}(\frac{P}{P_{ref}}) \quad (1)$$

Where:

L_p: is the sound pressure measured in dB.

P: is the root mean square (RMS) value of sound pressure measured in Pascals at a given distance from the sound source. If P exposes humans to extreme danger when reaches its maximum value of 200 Pascals.

P_{ref}: is the reference value of sound pressure which equals to 20 $\mu Pascals$ (0.0002 $\mu bars$).

It is worth to mention that L_p decreases by increasing the distance from the source level. Then the pressure level is given by Eq. (2):

$$P = P_{ref} 10^{\frac{L_p}{20}} \quad (2)$$

The noise pressure level is accompanied by a sound power radiated from the sound source; this power can be calculated using the formula in Eq. (3):

$$L_W = 10\ log_{10}(\frac{W}{W_{ref}}) \quad (3)$$

Where:

L_w: is the sound power level in dB.

W: is the power radiated by the sound source in Watts.

W_{ref}: is the reference power in Watts which equals (10^{-12}).

Consequently, the power level is given by Eq. (4):

$$W = W_{ref} 10^{\frac{L_W}{10}} \quad (4)$$

The threshold level that a human being can afford is 120 dB after which his health will be exposed to serious pain and damage. This threshold corresponds to a pressure of 20 Pascals and radiated power of 1 Watt.

A medium stone cutting factory was selected to measure the noise coming out of the cutting machines. A smartphone with an Android application was used to measure the noise pressure level in dB while moving away from the source of noise and taking readings. The measured values of distance and sound pressure levels varied from 94 dB at 0 m to 59.3 dB at 30 m, the complete results are shown in Figure 1. The pressure level in Pascals is calculated using Eq. (2) taking the measures of the values in dB and they are presented in Figure 1. The sound power radiated from the source will be dissipated as one moves away from the source. This power is calculated using Eq. (4) and it is shown in Figure 1.

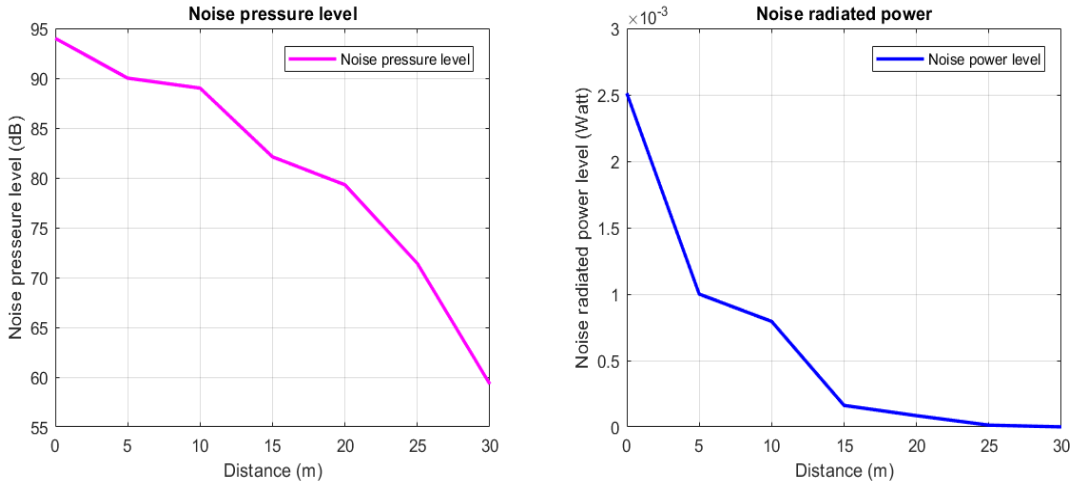

Fig. 1. Noise pressure level in (dB) and noise radiated power in (Watt) vs distance from source on (m).

3. Noise absorption, reflection, and isolation

Noise in stone cutting factories can be reduced and isolated in three different ways:

- Redesigning sound absorption walls for the barracks factory building.
- Installation of sound reflection barrier.
- Vibration isolation in stone cutting machines.

The selected stone cutting factory is a mixture of concrete and steel barracks house with W=20 *m* width, D=20 *m* depth, and H=10 *m* height as shown in Figure 2.

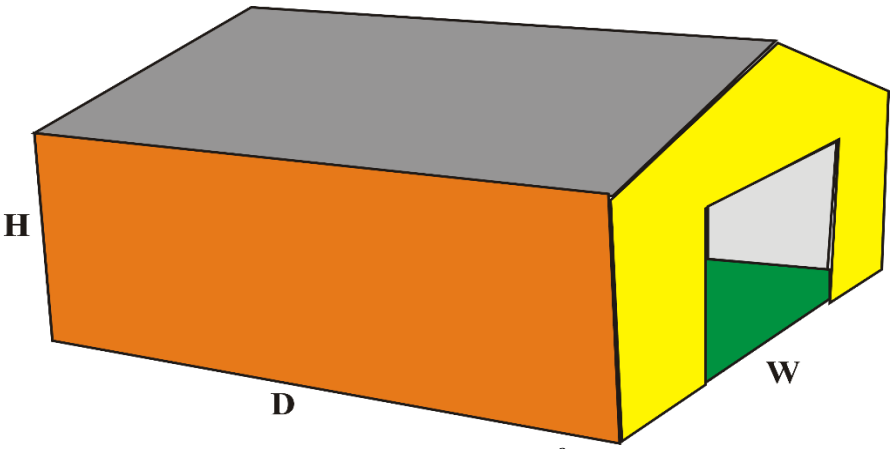

Fig. 2. Stone cutting factory (W X D X H m^3 barracks house).

The following three subsections will discuss the forgoing three options and techniques used for noise reduction, mentioning that the second technique related to the reflection barrier is used to protect the neighborhood houses from noise contamination but it has no positive influence on the workers working inside the cutting factory. On the other hand, the first and third techniques are related to the absorption walls and the machine vibration isolation has a significant effect in protecting the workers' health on one side and reducing the noise transmitted to the surrounding environment on the other side.

3.1 Sound absorption walls design

Looking at Figure 2, one can see that the selected barracks consists of two WXH m^2 and two DXH m^2 side concrete walls, one WXD m^2 the concrete floor and one WXD m^2 steel ceiling which forms the total surface area to be isolated using sound isolation material. The room sound absorption can be calculated by using Eq. (5) (ASHRAE, 2020):

$$S_a = \sum_{i=1}^{n} A_i \alpha_i \qquad (5)$$

Where:

S_a : The total room sound absorption.

A_i : The surface area of each wall.

n: The number of walls.

α_i : The absorption coefficient of each wall (depends on material and frequency).

According to ASHRAE (2020), the sound pressure level reduction can be calculated using the Eq. (6):

$$L_P = L_N + 10\, log_{10}\left(\frac{D}{4\pi r^2} + \frac{4(1-\alpha_m)}{S_a}\right) \qquad (6)$$

Where:

L_p : Sound pressure level received by the target in dB.

L_N : Sound pressure level produced from the machine in dB.

α_m : The average absorption coefficient.

D : The directivity coefficient.

r : The distance from the sound source.

The sound pressure level was simulated using Matlab Simulink to show the influence of the distance from sound source on the sound pressure level L_p in dB. The simulation was done first considering that the barracks is surrounded by steel sheets from the four walls and the ceiling while the floor is concrete which means that there is no absorption material on the walls. It is noticed from the green solid line in Figure 3 that in this case L_p drops to 93 dB in the first 10 *m* distance from the source and stayed still after that. The same

calculation has been done again using cork as a sound isolation material on the walls, it is clear from the violet dash-dot curve that L_p has dropped to 86 dB at a distance of 30 *m* while using concrete dropped L_p according to the orange dotted curve to 81 dB after 30 *m* and using asbestos dropped the red dashed curve to 77 dB after 30 *m*.

The best results have been obtained by using Rockwool material as a sound absorption material where the blue solid line in Figure 3 shows that the sound pressure has dropped to the level of 75 dB at a distance of 40 *m* from the sound source. The acceptable threshold sound level is about 80 dB which means that both asbestos and Rockwool can perform the required task but for health circumstances, it is recommended to use Rockwool. This calculation is based on using 50 *mm* thick (RwA 45) Rockwool fabricated in an equilateral triangular wedge shape as shown in Figure 4 to double the surface area and distract the reflected sound waves.

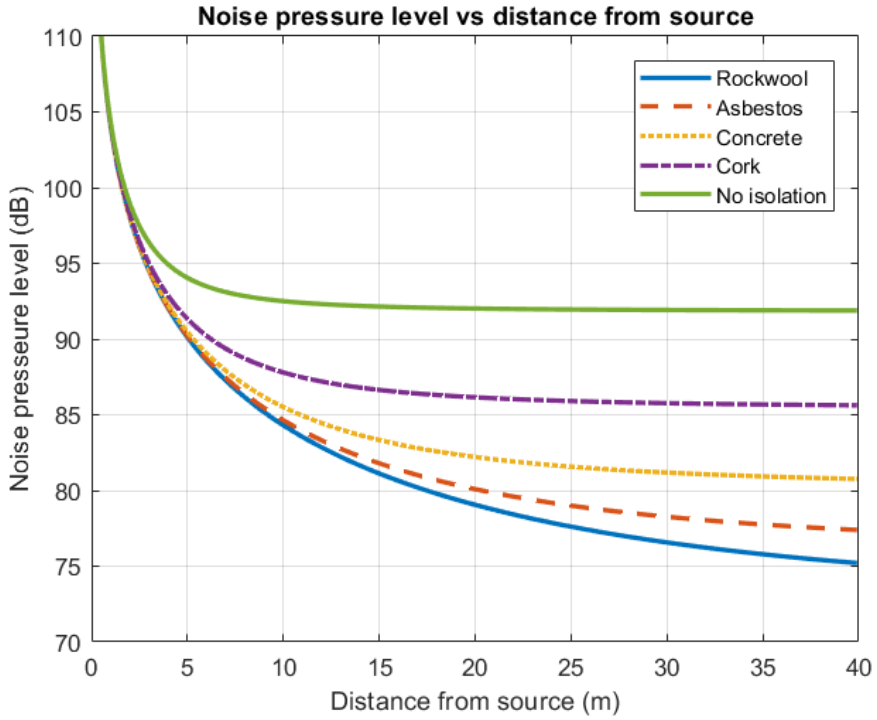

Fig. 3. Sound pressure level variation as a function of distance from the sound source and by using different types of sound isolation materials.

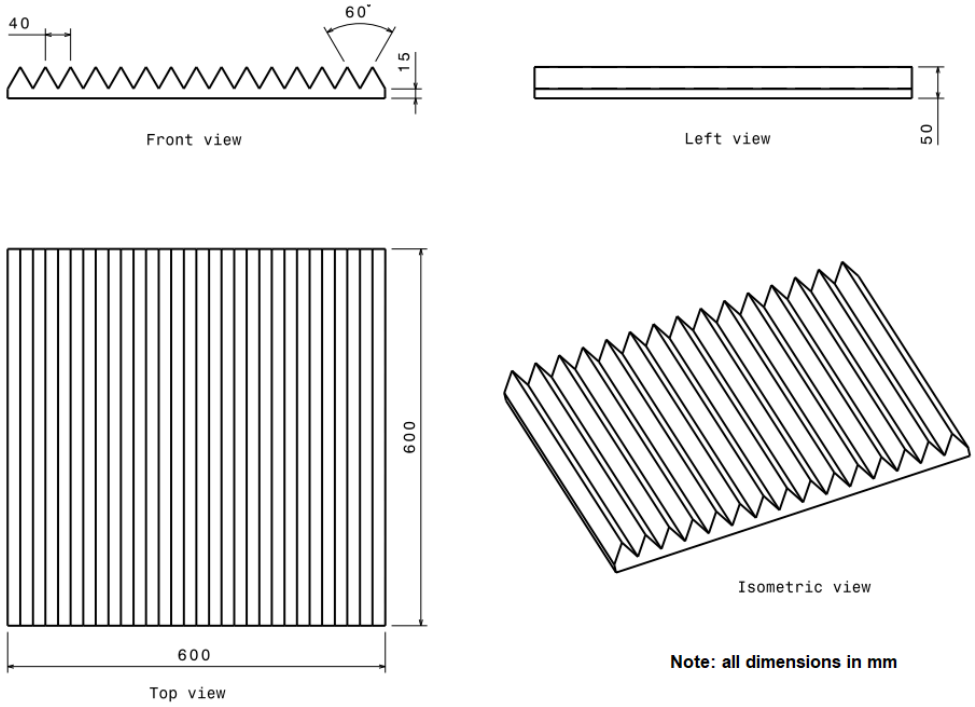

Fig. 4. Wedge-shaped Rockwool sound absorption material.

3.2 Sound reflection barrier design

The main entrance of each stone cutting factory includes a very wide gate that sometimes covers the whole wall from that side. This encounters a new sound pollution problem where noise can propagate from that gate outside to the neighborhood houses. This problem can be overcome by constructing a barrier wall at a specific distance from the sound source and with specific dimensions as shown in Figure 5.

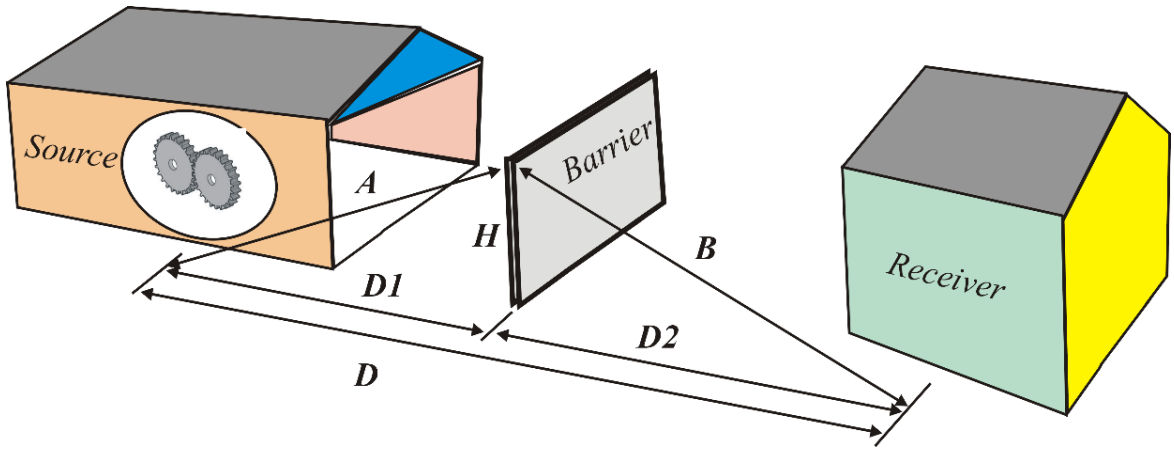

Fig. 5. Barrier construction for sound isolation between source and receiver.

Consider that there is a neighborhood populated house that we call here the receiver is located at a distance D from the main sound source which is a stone cutting machine. D equals to 70 *m* in the selected case study. Assume constructing a concrete barrier with a height H between the source and receiver at a distance of D_1 from the source to the bottom of the barrier and A to its top. The receiver is located at a distance D_2 from the bottom of the barrier and B from its top. It is required her to estimate the height of the barrier H and its distance from the source D_1. The Path Length Difference (PLD) can be calculated by using Eq. (7):

$$PLD = A + B - D \quad (7)$$

If the required attenuation in the sound pressure level between the source and the receiver is 20 dB at 4000 Hz, PLD can be selected from ASHRAE sound and noise tables (ASHRAE, 2020) to be equal to 0.5. In the selected case study, the barrier can be located at a distance D_2 equals to 40 *m* limited by land borders. Referring to Figure 5 and based on geometry calculations the height of the barrier that gives this attenuation (20 dB) equals to 4.25 *m*.

3.3 Vibration isolation of stone cutting machine

The third technique proposed to reduce the noise-induced by a stone cutting process is by reducing and isolating the vibrations produced in the cutting machine during the cutting process. Noise results from the impact between the teeth of the cutting disk and stone. Each revolution of the disk contains a specific number of teeth, this implies that the disturbance vibration frequency in Hz equals to the number of revolutions per second multiplied by the disk number of teeth. The cutting disk is connected to the electric driving motor through a rotating shaft as shown in Figure 6. The vibration isolation interface is placed between the motor and the holding bridge.

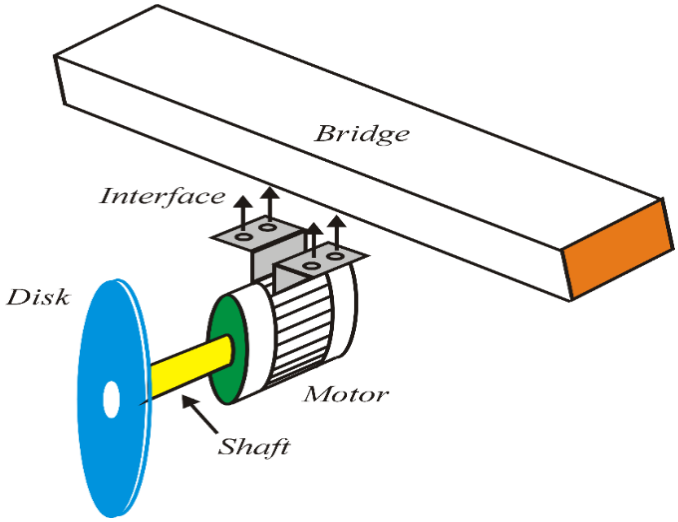

Fig. 6. Technical drawing of the motor and cutting disk

To analyze the vibrations in a good manner it is necessary to calculate the resultant cutting force (F_D). According to Turchetta (2010) , the first step is to calculate the equivalent chip thickness (h_{eq}) by using Eq. (8). In this paper, the worst scenario is selected from (Turchetta, 2010) to compute (F_D) due to the absence of experimental results because of COVID-19 pandemic and lack of movement. Based on that, the cutting depth (d_p) is 0.5 mm, the feed speed (v_a) is 600 mm/min, and the cutting speed (v_t) is 2000 rpm as used in Turchetta (2010). Therefore, h_{eq} is $2.6525 * 10^{-4}$ *mm*.

$$h_{eq} = \frac{d_p v_a}{v_t} \tag{8}$$

Where:

d_p: the cutting depth.
v_a: Feed speed.
v_t: Cutting speed.

The second step is to compute the traverse cutting force (F_T) and the radial cutting force (F_R) respectively. This is achieved by using Eqs (9) and Eq. (10) as shown below (Turchetta, 2010)

$$F_T = 111.h_{eq}^{0.217} \tag{9}$$

$$F_R = 121.h_{eq}^{0.236} \tag{10}$$

Where:

h_{eq}: The equivalent chip thickness.

The treverse cutting force (F_T) is equal to 18.59 N while the radial cutting force (F_R) is equal to 17.33 N. Finally the resultant disturbance cutting force (F_D) is equal to 25.41 N while it is direction (β) is 50°. For more information see (Turchetta, 2010, Tlusty, 2000).

The whole system has been modeled as a Finite Element Model (FEM) using CATIA software. Figure 7 shows the FEM results of the cutting disk where displacement

is seen in Figure 7 (c) on the bottom while on the right one (Figure 7 (b)) one can see the Von Mises stress effect of the cutting force. Figure 8 shows the Von Mises stresses on the outermost surface of the shaft in the static analysis as well.

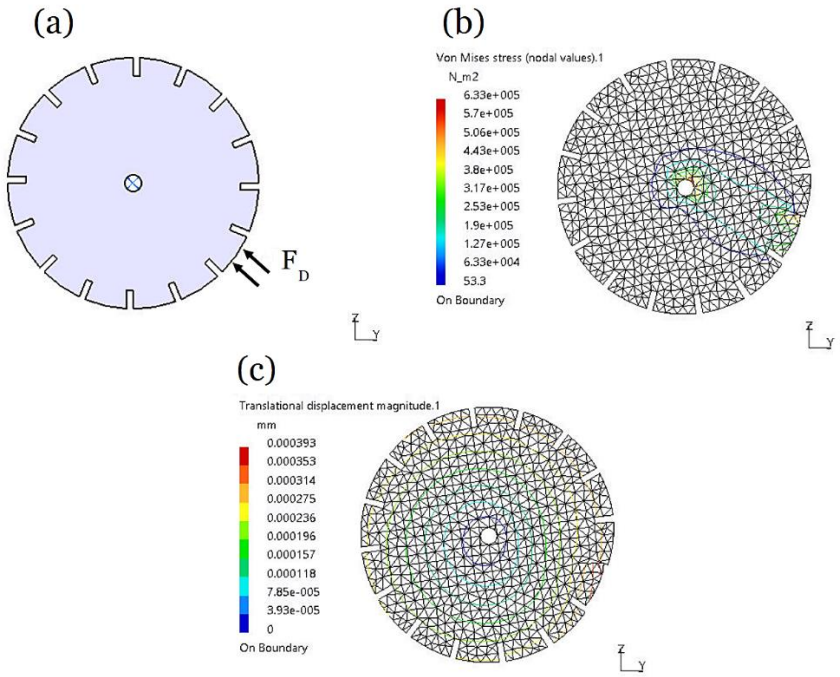

Fig. 7. The analysis of the cutting disk from the static FEM in CATIA software a) Conditions of the test b) Von mises stress test c) Translation displacment magnitude test.

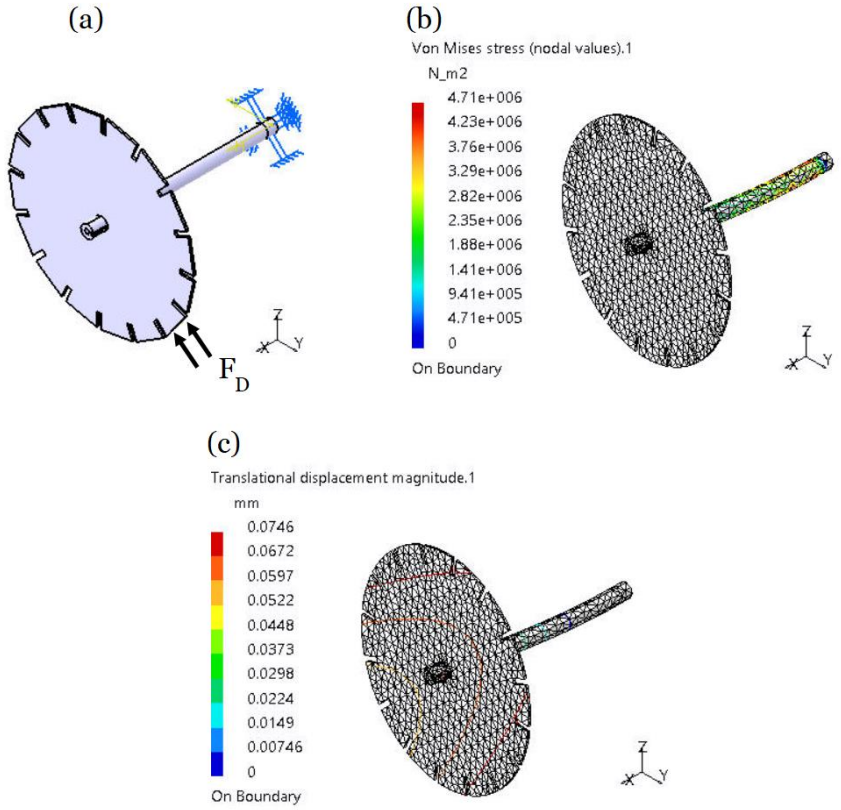

Fig. 8. The analysis of the shaft from the static FEM in CATIA software a) Conditions of the test b) Von mises stress test c) Translation displacment magnitude test.

The dynamic frequency analysis for the system on CATIA has been executed to test the vibrational behaviour, the resulting modes and mode shapes are as shown in Figure 9. The first and second modes have the same natural frequency 67 Hz almost because these are the lateral bending modes taken by fixing the interface and the third mode is the rotational mode of the disk and shaft at 102 Hz. There are other modes at much higher frequencies but they were neglected because they can be isolated by the interface at high frequency.

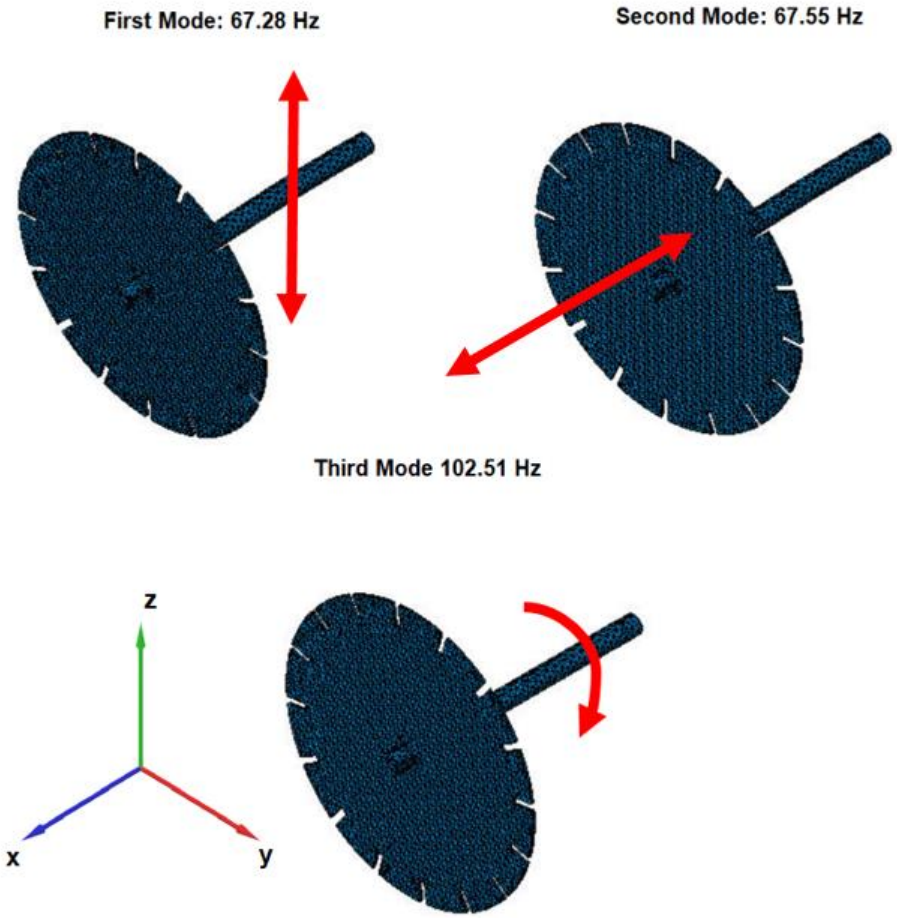

Fig. 9. Vibration modes resulted from the dynamic frequency analysis on CATIA.

The mathematical model has been derived for the system for more validation as depicted in the schematic drawing in Figure 10. In this Figure, the disk mass is represented by the mass m_d and the motor mass is the mass M. The disk is connected to the motor by a shaft that has a stiffness value K_1 (damping is neglected here) and the motor is connected to the bridge through the interface with a stiffness K_2 and the damping coefficient C_2. The main disturbance force is the cutting force on the disk F_D. While F_a is added to the model to represent the force of the actuator in the case of using active control for the vibrations.

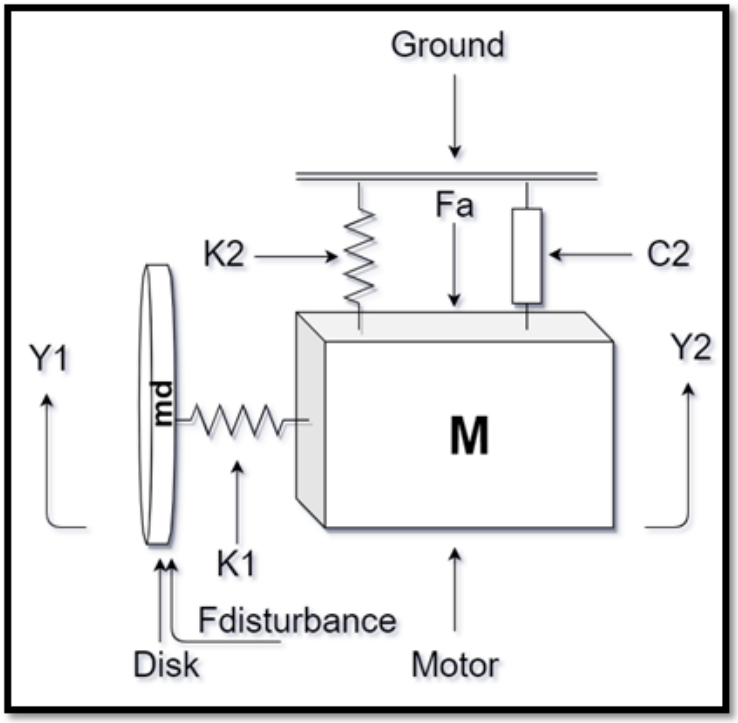

Fig. 10. Schematic drawing of the system for the mathematical model.

From the schematic diagram in Figure 10 and using Newton's second low Eq. (11) represents the Eq. of motion for the disk:

$$\ddot{Y}_1 = \frac{F_D}{m_d} + \frac{K_1}{m_d} Y_2 - \frac{K_1}{m_d} Y_1 \tag{11}$$

Where: Y_1 is the displacement of the disk, Y_2 is the displacement of the motor, $\ddot{Y}_1$ is the acceleration of the disk and F_D disturbance force due to the cutting process. From the diagram in Figure 10 and using Newton's second low Eq. (12) represents the equation of motion for the motor:

$$\ddot{Y}_2 = \frac{(-K_1 - K_2)}{M} Y_2 - \frac{C_2}{M} \dot{Y}_2 + \frac{K_1}{M} Y_1 - \frac{F_a}{M} \tag{12}$$

Where: Y_1 is the displacement of the disk, Y_2 is the displacement of the motor, $\dot{Y}_2$ is the velocity of the motor, $\ddot{Y}_2$ is the acceleration of the motor and F_a the actuator force applied on the motor by active control. The state-space approach has been used to represent this model taking the variables x=$[Y_1, Y_2, \dot{Y}_1, \dot{Y}_2]^T$ as the state variables of the system. The output force transmitted from the motor to the bridge F is measured by Eq. (13):

$$F = K_2 Y_2 + C_2 Y_2 + F_a \tag{13}$$

Therefore, the state space representation is given by E. (14):

$$\begin{aligned} \dot{x} &= Ax + B F_a + B_d F_D \\ y &= Cx + D F_a \end{aligned} \tag{14}$$

$$[A] = \begin{bmatrix} 0 & 1 & 0 & 0 \\ -\frac{K_1}{m_D} & 0 & \frac{K_1}{m_D} & 0 \\ 0 & 0 & 0 & 1 \\ \frac{K_1}{M} & 0 & \frac{(-K_1-K_2)}{M} & -\frac{C_2}{M} \end{bmatrix} \quad , \quad [B] = \begin{bmatrix} 0 \\ 0 \\ 0 \\ -\frac{1}{M} \end{bmatrix}$$

$$[B_d] = \begin{bmatrix} 0 \\ \frac{1}{m_D} \\ 0 \\ 0 \end{bmatrix} \quad , [C] = \begin{bmatrix} 1 & 0 & 0 & 0 \\ 0 & 0 & 1 & 0 \\ 0 & 0 & (K_2 + C_2) & 0 \end{bmatrix}, \quad [D] = \begin{bmatrix} 0 \\ 0 \\ 1 \end{bmatrix}$$

Where:

$A \in R^{4*4}$: is the system matrix.
F_a : is the input force where it is the actuator force applied on the motor.
F_D: is the disturbance input due to the cutting process.
$B \in R^4$: is the force input vector.
$B_d \in R^4$: is the disturbance force input vector.
$C \in R^{3*4}$: is the output matrix.
$D \in R^3$: is the feedforward vector.

Figure 11 shows the transmissibility frequency response function (FRF) of the system taking the disturbance cutting force F_D as an input and the transmitted force F from the motor to the bridge as an output. This transfer function shows the first two modes of the system where the first frequency at 67 Hz is the lateral bending mode of the shaft and the second mode at a frequency of 102 Hz.

The FRF was calculated once by considering that the motor is bolted directly with a flexible metallic interface to the bridge without any damping (this is shown in blue solid line). The second time the FRF was calculated with inserting an elastomeric rubber pad between the motor and bridge with a stiffness K_2 and damping C_2. This introduced passive damping to the system causing the overshoots to drop about 30 dB (the dashed red line).

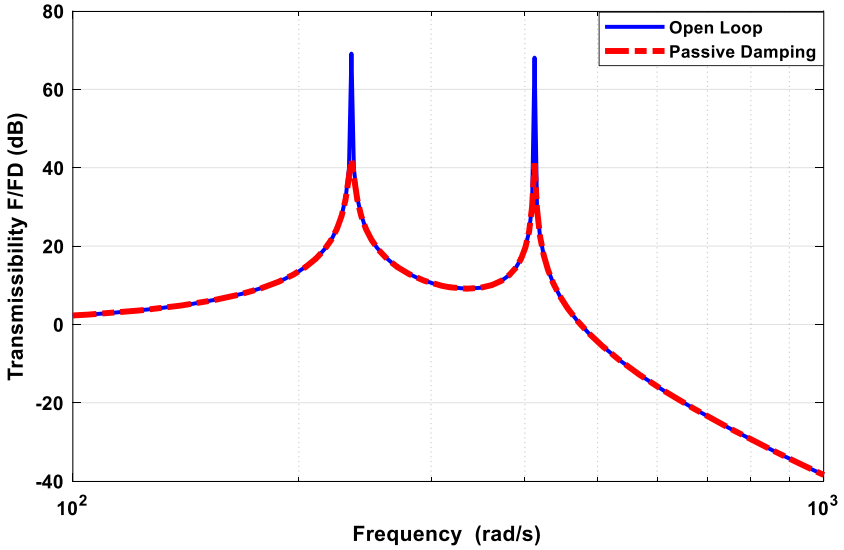

Fig. 11. Transmissibility frequency response function between the cutting force as an input and the transmitted force to the bridge as an output. This comparison between the open-loop system and the system with passive damping.

The last option to damp and isolate vibrations transmitted from the motor and disk to the bridge and base of the machine is by using active damping. This technique is done by inserting a force sensor collocated with a force actuator between the motor and the bridge; the force sensor measures the transmitted force from the motor to the bridge

and the signal is fed back to the actuator through a simple integrator as a compensator. This technique is called Integral Force Feedback (IFF) (Preumont, 2002), it proved robustness and good performance in active control of mechanical structures. The active force is computed by Eq. (15):

$$F_a(s) = g\frac{1}{s}F(s) \qquad (15)$$

Where:

F_a(s) :is the control force.
g : is the gain of the control action.
F (s): is the transmitted measured force.

Figure 12 shows the root-locus plot of the closed-loop system, the poles and zeros of the system are alternating because of the collocation of the sensor and actuator which helps to obtain stability and high control authority. When increasing the gain of the controller each pole migrates towards the adjacent zeros and all stay in the left side plane of the plot, but it is clear that the influence of the controller on the first mode is much higher than that on the second mode. Figure 13 depicts the transmissibility frequency response function between the transmitted force to the bridge and the disturbance force on the disk. The figure compares between the open-loop (dashed blue line) and the closed-loop (red solid line). This result is achieved when the gain g = 80. The performance is much better than using passive mount only where the overshoot of the first mode has almost vanished and the second mode was reduced more than 45 dB.

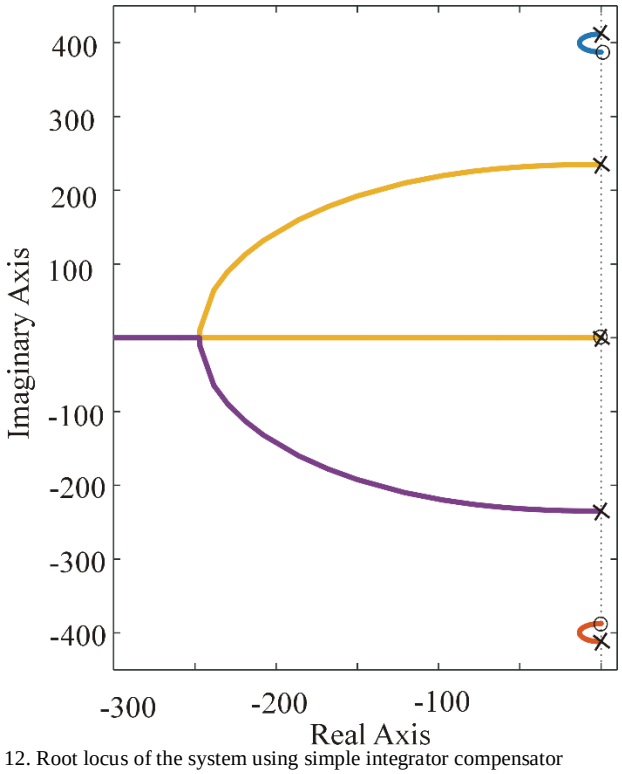

Fig. 12. Root locus of the system using simple integrator compensator

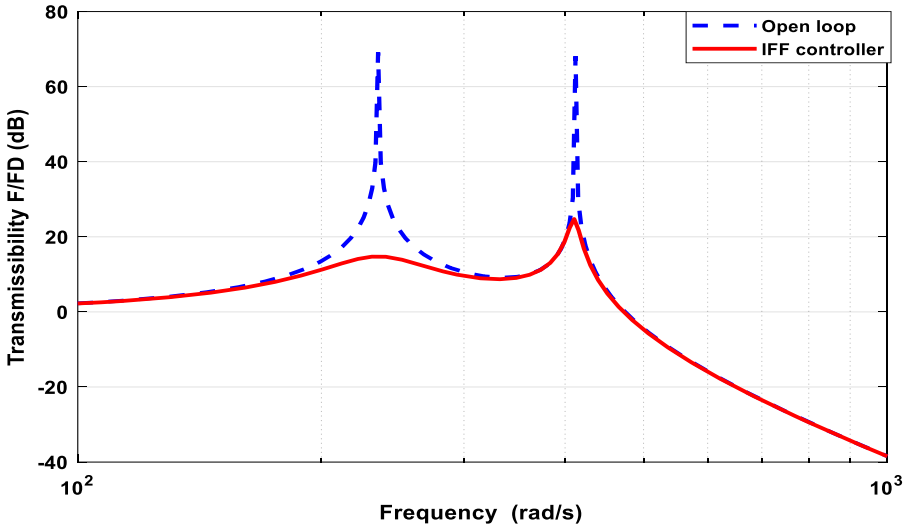

Fig. 13. Transmissibility frequency response function between the cutting force as an input and the transmitted force to the bridge as an output (active damping). This comparison between the open-loop system and the system with the IFF controller.

Another technique is used to decrease the amplitude of the vibrations or kill the vibrations if it is possible in the cutting stone. This technique is focused on building a regulator based on LQR to perform the required task. The control scheme is shown in Figure 14 while the control action is given by Eq. (16) (Ogata and Yang, 2002).

$$F_a(t) = -Kx(t) \tag{16}$$

Where:

$F_a(t)$: is the input force where it is the actuator force applied on the motor.
$K \in R^4$: is the gain matrix.
$x(t) \in R^4$: is the state vector.

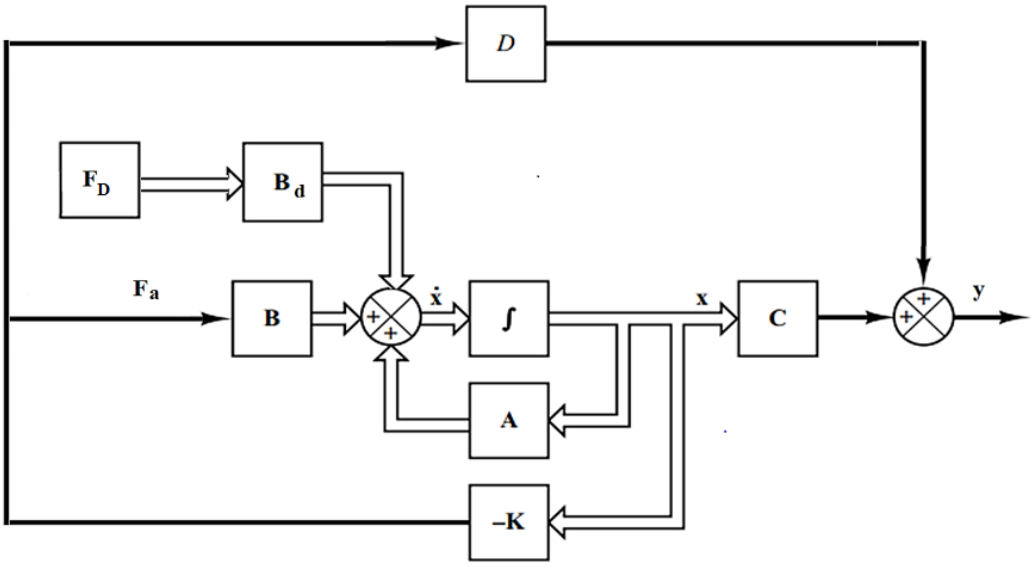

Fig. 14. The regulator scheme based on LQR for the stone cutting machine.

Consequently, the closed-loop dynamics of the regulator can be computed by substituting Eq. (16) into Eq. (14). Therefore, the result is shown in Eq. (17).

$$\begin{aligned} \dot{x} &= (A - BK)x + B_d\, F_D \\ y &= Cx - D\, Kx \end{aligned} \tag{17}$$

Where:
$A \in R^{4*4}$: is the system matrix.
F_a : is the input force where it is the actuator force applied on the motor.
F_D: is the disturbance force input due to the cutting process.
$B \in R^{4*1}$: is the force input vector.
$B_d \in R^{4*1}$: is the disturbance force input vector.
$C \in R^{3*4}$: is the output matrix.
$D \in R^3$: is the feedforward vector.

According to [17], the LQR is an advanced control method to compute the optimal control action for minimizing the cost function concerning the dynamics of the system which is shown in Eq. (18). This optimization problem is classified as Quadratic Programming (QP) problem so by selecting proper values for the weighting matrices Q and R the optimal gain matrix (K) can be computed. Usually, to compute the optimal gain matrix it is necessary to solve the Reduced Algebraic Riccati Equation for more information see [18]. Therefore, the optimal gain matrix (K) is computed by using MatLab see Eq. (19).

$$\begin{aligned} J(u) &= \int_0^\infty (x(t)^T Q x(t) + F_a(t)^T R\, F_a(t))\, dt \\ &\text{Subjected to:} \\ \dot{x}(t) &= Ax(t) + B\, F_a(t) \end{aligned} \tag{18}$$

Where:
$Q \in R^{4*4}$: is a semi-positive definite matrix or positive definite matrix.
R: is a positive definite matrix.

$$K = lqr(A, B, Q, R) \tag{19}$$

It is important to mention the effect of increasing the Q matrix that means the closed-loop eigenvalues are shifted more to the left on the s-plane and vice versa, i.e. increasing Q means that the priority is to enhance the performance of the system rather than increasing the energy saving. On the contrary, increasing the R matrix has the opposite effect of increasing the Q matrix (Ogata and Yang, 2002, Kirk, 2004).
In the following results, Q and R are selected as shown below

$$Q = 1000 * \begin{bmatrix} 1 & 0 & 0 & 0 \\ 0 & 1 & 0 & 0 \\ 0 & 0 & 1 & 0 \\ 0 & 0 & 0 & 1 \end{bmatrix}, R = 0.001$$

The FRF is computed for all the presented techniques to compare among them and to determine which one is more suitable to use it on the real prototype. The results are shown in Figure 15 so the passive damping technique succeeded to reduce the transmissibility up to 30 dB while IFF controller can reduce the transmissibility up to 45 dB. But the most effective technique among all the presented techniques is to design a regulator based on LQR because the transmissibility decreases up to 54 dB. But the LQR corresponds to the reduction of high frequency attenuation which reduces its performance at high frequency.

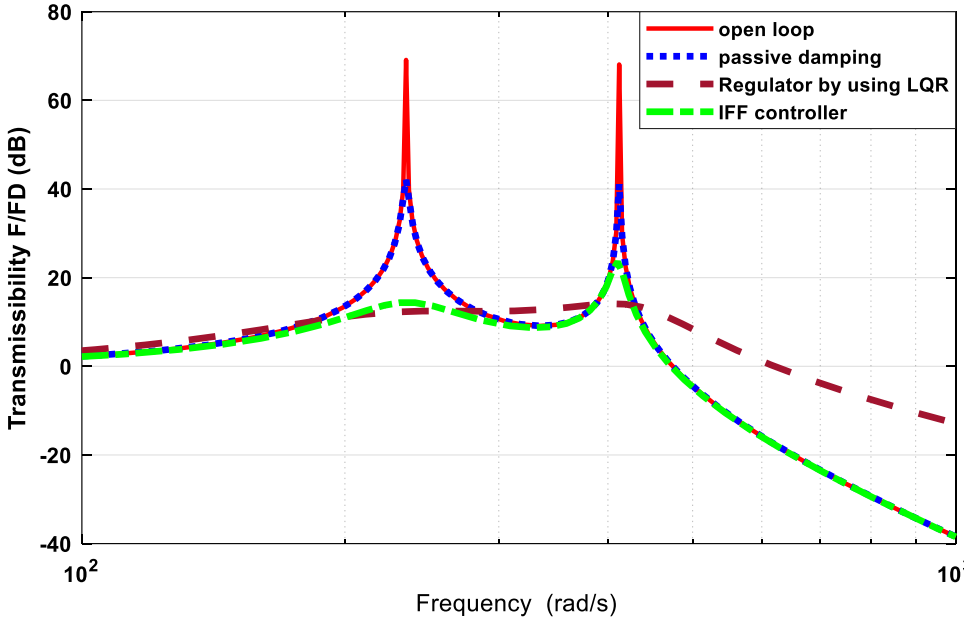

Fig. 15. Transmissibility frequency response function between the cutting force as an input and the transmitted force to the bridge as an output. This comparison between the open-loop system, the system with passive damping, the system with integration with IFF controller, and the system with integration with LQR.

4. Conclusions and Future Work

This research has been conducted for its importance and high influence on human beings living around stone-cutting factories. The noise produced from these factories makes high sound pollution in the surrounding environment causing severe health influence. Three techniques were proposed in this article to overcome noise and to solve this problem. The first technique is summarized by adding a thickness of sound-absorbing material to the walls of the factory barracks, this absorbing material helps in reducing the effect of sound inside the factory and outside it to protect workers and neighbourhood people. The second technique is done by constructing a barrier concrete wall between the factory and the populated houses, this barrier helps to reflect noise away from surrounding people but it does not influence workers inside the factory. The third technique is a seminal one because it can be done by damping and isolating vibrations induced from the stone cutting machine during the cutting process which is the main source of the noise. This helps in reducing the source of noise, thus, it has a positive effect on both internal workers and external neighbours. It is recommended for each stone cutting factory to use one or more of these techniques to increase the sustainability of their factories and increase their contribution to environmental sound pollution reduction.

References

[1] Jaber H, Mohamed M, El-Safty A, El-Salamoni O and Ibrahim H (2015) Prevalence and Risk Factors of Noise Induced Hearing Loss and other Work-Related Health Problems among Stone Saw Workers in West Bank-Palestine. *Med. J. Cairo Univ* 83(2).

[2] Kylen P, Stjernvall JE and Arlinger S (1977) Variables affecting the drill-generated noise levels in ear surgery. *Acta oto-laryngologica*, 84(1-6): 252–259.

[3] Aleksandrova AJ, Timofeeva SS (2017) *Risk Assessment for Stonecutting Enterprises*. Tomsk, Russian Federation.

[4] Jenkins MD, Nelson PA, Pinnington RJ, and Elliott SJ (1993) Active isolation of periodic machinery vibrations. *Journal of Sound and Vibration* 166(1): 117–140.

[5] Scribner KB, Sievers LA and von Flotow AH (1993) Active narrow-band vibration isolation of machinery noise from resonant substructures. *Journal of Sound and Vibration*, 167(1): 17–40.

[6] Delibalta MS, Kahraman S and Comakli R (2015) The usability of noise level from rock cutting for the prediction of physico-mechanical properties of rocks. *Fluctuation and Noise Letters* 14(01).

[7] Jeon JY, Jeong JH and Ando Y (2002) Objective and subjective evaluation of floor impact noise. *Journal of Temporal Design in Architecture and the Environment* 2(1): 20.

[8] Sykes AO and Harrison M (1952) On the Use of Metallic Noise Isolation Mounts. *The Journal of the Acoustical Society of America* 24(1): 117.

[9] Goodfriend LS (1963) Lead as a Ceiling Barrier for Sound. *The Journal of the Acoustical Society of America* 35(5): 785.

[10] Al-Joulani N (2008) Soil Contamination in Hebron District Due to Stone Cutting Industry. *Jordan Journal of Applied Science* vol 10: 37–50.

[11] Sayara T (2016) Environmental impact assessment of quarries and stone cutting industries in Palestine: case study of Jammain. *Journal of Environment Protection and Sustainable Development* 2(4): 32–38.

[12] Jie KL, Yung TC, Hao KY and Huann GY (2017) Numerical analysis of transmission loss through various noise barrier. *Proceedings of the International Conference on Vibration, Sound and System Dynamics*, Penang.

[13] ASHRAE Noise & Vibration Control, Inc. (2020) *HVAC Noise & Vibration Control: RTU Best Practices*. Available at: http://www.brd-nonoise.com (accessed: 18 March 2020).

[14] Turchetta S (2010) Cutting force in stone machining by diamond disk. *Advances in Materials Science and Engineering*.
[15] Tlusty G (2000) *Manufacturing Processes and Equipment*: Prentice-Hall.
[16] Preumont A (2002) *Vibration control of active structures: an introduction: Kluwer Academic Publishers*.
[17] Ogata K and Yang Y (2002) *Modern control engineering*: Prentice hall, India.
[18] Kirk DE (2004) *Optimal control theory: an introduction*: Courier Corporation.